PERGAMON

Journal of Structural Geology 26 (2004) 177–196

JOURNAL OF STRUCTURAL GEOLOGY

www.elsevier.com/locate/jsg

Correlating deformation in Variscan NW-Iberia using porphyroblasts; implications for the Ibero-Armorican Arc

Domingo G.A.M. Aerden*

Departamento de Geodinámica, Universidad de Granada, C/Fuenteneuva s/n, 18071 Granada, Spain

Received 27 January 2002; received in revised form 13 March 2003; accepted 17 March 2003

Abstract

3-D microstructural analysis of 30 porphyroblastic samples from the Variscan orogen in NW-Iberia has revealed four sets of inclusion trails with distinctive geographic trends and relative timing. The chronological and orientational consistency of these microstructures provides a reference frame for the correlation of macroscopic structural successions. The two younger inclusion trail sets correlate with the main map-scale structures of Middle- to Upper-Carboniferous age, whereas the two older sets correspond to mesoscopic structures preserved locally in low-strain pods, and dating back as far as 365 Ma (Upper Devonian). Inclusion trail orientations appear uninfluenced by a major orocline in the study area (Ibero-Armorican Arc) outlined by late-stage folds and thrusts with variable trends. It is proposed that the orocline developed by WNW–ESE-trending transpression superposed on originally N–S to NE–SW-trending structures during a late stage of the orogeny (Upper-Carboniferous). Domains of low- or zero-strain (e.g. porphyroblasts) are inferred to have maintained relatively constant orientations in the zone of transpression, presumably due to deformation partitioning effects. Consequently, they preserve a succession of pre-orocline structural trends. The collected microstructural data also indicate moderate preferred vertical and horizontal orientations of inclusion trails in the analysed samples as reported earlier in other Variscan regions. This probably witnesses a dynamic equilibrium between tectonic forces and gravity during four periods of differently oriented crustal shortening that generated the four recognised sets of inclusion trails.

Keywords: Porphyroblast; Inclusion trails; Orocline; Iberian Massif; Ibero-Armorican Arc

1. Introduction

Correlating local structural successions is a difficult but important component of reconstructing the tectonic evolution of an orogenic belt. Difficulties commonly arise from (1) discontinuous preservation of early-formed fabrics and structures that appear partially transposed by younger ones, and (2) reactivation of early-formed fabrics during later deformation with consequent loss or modification of their original kinematic signature. Recently, a new microstructural approach for structural correlation has been applied in different orogens based on the discovery of regionally consistent orientations of inclusion trails in complexly folded rocks and regions (e.g. Johnson, 1990; Bell et al., 1992, 1999; Aerden, 1994, 1998; Stallard, 1998; Bell and Mares, 1999; Hickey and Bell, 1999; Jung et al., 1999). This consistency enables successive foliations with distinctive orientations to be recognised, dated (cf. Bell and Welch, 2002) and followed over large distances, despite heterogeneous and discontinuous preservation.

This article documents relationships between inclusion trails and macroscopic structures in NW-Iberia where Variscan crustal deformation progressively migrated from internal to external orogenic zones between approximately 390 and 290 Ma (Dallmeyer et al., 1997). Despite this diachronous evolution, two or three deformation phases have been consistently recognised throughout the study area. However, the correlation of these phases, and their tectonic significance have remained uncertain, due to intervening major shear zones that juxtapose different crustal segments. Apart from this problem, prograde metamorphic structures and fabrics, in the higher-grade areas, have been extensively reactivated and transposed during their exhumation. Consequently, few kinematic constraints exist on the early-orogenic evolution of the

* Tel.: +349-5827-2883; fax: +349-5824-8527.
E-mail address: aerden@ugr.es (D.G.A.M. Aerden).

0191-8141/03/$ - see front matter © 2003 Elsevier Ltd. All rights reserved.
doi:10.1016/S0191-8141(03)00070-1

Iberian Massif. It will be shown that analysis of porphyroblast microstructures can help solve these problems by providing unique insight into the early deformation history of individual rocks and the study area as a whole.

Thirty prophyroblastic samples spanning a distance of more than 300 km have been analysed using recently developed 3-D microstructural techniques and reveal structural paths of unsuspected complexity. This microstructural work has been combined with new structural mapping of a key area, and a review of existing structural data.

2. Geological setting

The European Variscan orogen developed during the Devono-Carboniferous collision of Gondwana, Armorica and Laurentia (Matte, 2001). Extensional tectonics during the Mesozoic and Cainozoic resulted in the present fragmentary exposure of the belt in a number of isolated massifs. The Iberian Massif is the largest of these massifs (Fig. 1) and preserves a complete cross-section through the orogen, which exhibits a bilateral symmetry. Two external fold and thrust belts involving Cambrian to Upper-Carboniferous strata are observed, separated by a 400-km-wide internal zone containing strongly deformed, medium- to high-grade rocks of mostly Uppermost-Proterozoic to Silurian age, intruded by syn- and late-orogenic granitoids.

An important feature of the internal zones is a high-grade nappe complex preserved as five tectonic klippen known as the Cabo-Ortegal, Ordenes, Malpica-Tuy, Bragança and Morais allochthonous complexes (Ribeiro et al., 1990; Fig. 1). The allochthonous nature of these rocks is indicated by lithostratigraphy (abundant mafic and ultramafic rocks), high-pressure metamorphism, and distinctive geochemical signatures. The general structure of the nappe complex is simple and of great lateral continuity. Three principle units can be distinguished: the Basal Unit, Ophiolitic and Upper Units (terminology of Martínez Catalán et al., 1996). The Basal Unit is composed of Silurian metapelites, orthogneisses and mafic bodies, and is generally interpreted as an originally deeply subducted portion of the continental margin of Gondwana (Arenas et al., 1995; Martínez Catalán et al., 1996). The overlying Ophiolitic Unit comprises metamorphosed fragments of oceanic crust (mostly metagabbro and amphibolite) and related metasediments, which are probably derived from the Rheic Ocean (Variscan Ocean). The Upper Unit comprises a lower sub-unit composed of medium- to high-pressure (ultra)mafic eclogites, granulites and felsic orthogneisses, which is tectonically overlain by a thick pile of medium- to low-grade Cambro-Ordovician metapelites. Based on their structural position above the Ophiolite and geochemical evidence, the Upper Unit is generally interpreted as a fragment of non-Iberian lower crust (e.g. Ribeiro et al., 1990). The three allochthonous units are carried by a more continuously exposed para-autochthonous nappe (Galicia-Tras-os-Montes Zone; GTMZ) containing mainly Silurian slates and quartzites. The main contacts between the nappes are subhorizontal, brittle-ductile shear zones, which have been moderately folded with subvertical axial planes. However, internally, individual nappe units exhibit evidence for a complex deformation history prior to and during nappe emplacement. The main fabrics and structures observed in the field developed during progressive exhumation and retrogression of these rocks, but prograde assemblages and fabrics are locally preserved in low strain domains and in porphyroblasts.

Most of the Iberian Massif is composed of the autochthonous footwall of the allochthonous nappes, and is traditionally subdivided into five zones with different palaeogeographic significance (Fig. 1). The Central Iberian Zone is composed of low- to high-grade Upper-Proterozoic to Lower-Devonian metasediments and abundant syn- and post-orogenic granitoids. The dominant structures are upright folds cut by low-angle extensional shear zones and thrusts. The West-Asturo-Leonese Zone and Ossa Morena Zone occupy intermediate positions on opposite sides of the Central Iberian Zone, and contain large recumbent fold nappes that have been refolded about steep axial planes. The external Cantabrian Zone and South Portuguese Zone show thin-skinned thrust tectonics affecting Upper-Proterozoic to (synorogenic) Upper-Carboniferous Flysch and Molasse-type deposits. The contacts between the Central Iberian Zone and Ossa Morena Zone and between the latter zone and the South Portuguese Zone are marked by strongly deformed rocks containing lenses of high-grade mafic and ultramafic rocks similar to those found in the allochthonous complexes (Fig. 1). Both contacts are interpreted as sutures and possible root zones of the allochthonous complexes.

3. Sample description

Of about 80 porphyroblastic samples collected from the Basal Unit, para-autochthonous unit, and the Central Iberian Zone, 30 contained inclusion trails of sufficient quality to be further analysed (see Fig. 1 for sample locations). Nineteen samples from the Basal Unit include 17 albite–garnet schists, one retrograded eclogite from a mafic lens (sample 2), and one sample of staurolite–andalusite schist (sample 21). Albite and garnet porphyroblasts in these rocks preserve prograde assemblage inclusions (quartz, muscovite, garnet, epidote, rutile, ilmenite) recording metamorphic conditions of 575 °C and 1500 MPa (Arenas et al., 1995) for the most deeply exhumed parts of the Basal Unit represented by samples 1–5. The matrix of these samples reequilibrated to muscovite, chlorite, quartz, epidote, and ilmenite during exhumation and nappe formation under amphibolite to greenschist facies conditions. The eclogite sample contains sigmoidal and spiral-shaped inclusion trails of sphene preserved within garnet porphyroblasts, and the matrix is completely retrograded to green amphibole,

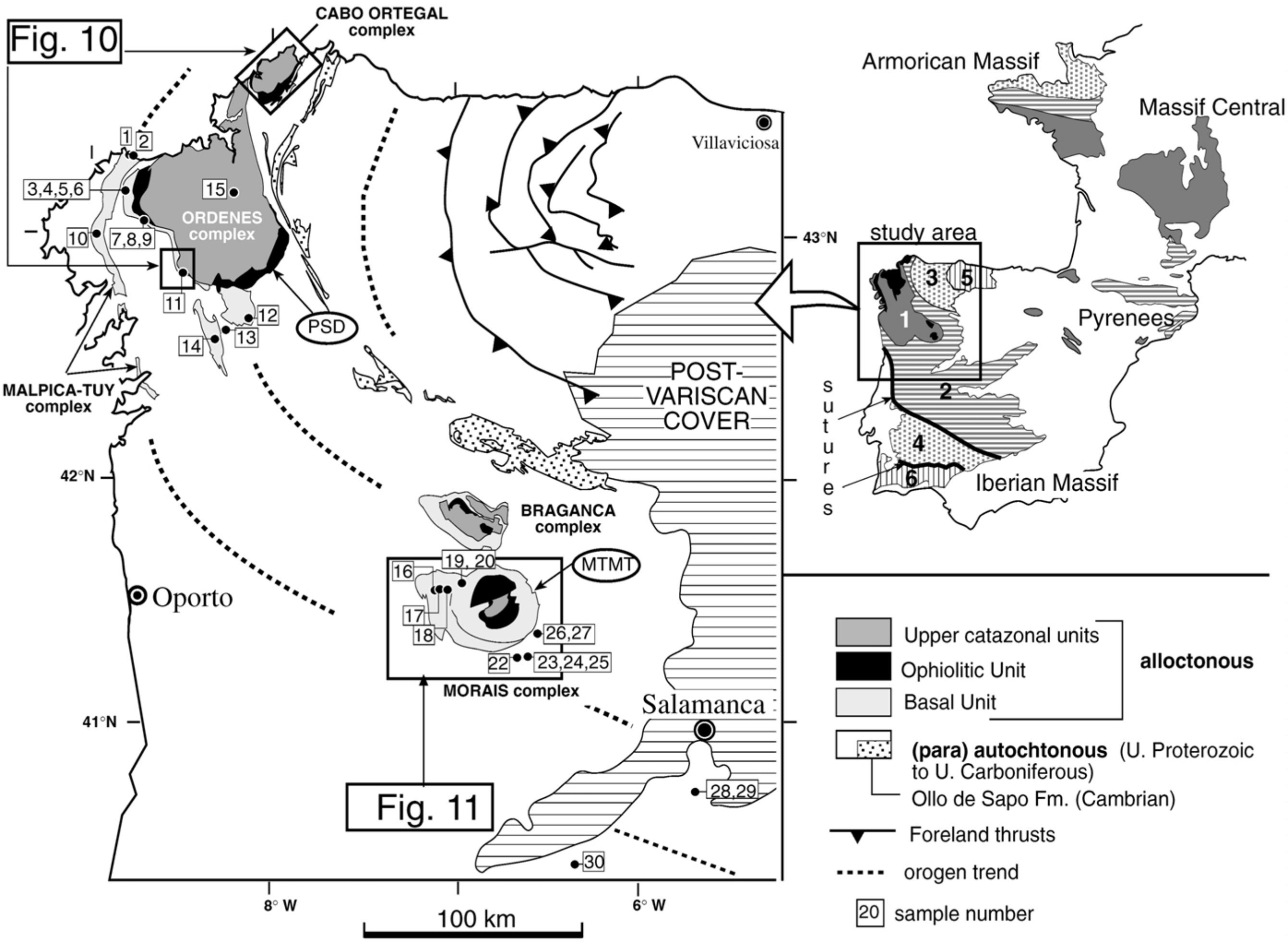

Fig. 1. Simplified geological map of NW-Iberia showing the locations of analysed samples. PSD = Pico Sacro Detachment; MTMT = Main Tras-os-Montes thrust. 1: Galicia-Tras-os-Montes Zone with allochthonous klippen in black. 2: Central-Iberian Zone. 3: West-Asturo-Leonese Zone. 4: Ossa-Morena Zone. 5: Cantabrian Zone. 6: South-Portuguese Zone.

clinozoisite and sphene. Sample 13 was collected from the highly sheared uppermost zone of the para-autochthonous nappe unit, but shows identical petrographic and microstructural features to the Basal Unit samples. One garnet-schist sample from the higher metapelitic part of the Upper Unit in the Ordenes Complex (sample 15) was also included in the analysis. Nine analysed samples from the Central Iberian Zone (autochthonous) were collected south-east of the Morais complex (Fig. 1), and are Cambro-Ordovician metapelites containing andalusite, staurolite, and/or cordierite porphyroblasts.

4. Quantitative microstructural data

4.1. Computer analysis of inclusion trail orientations

Variably oriented vertical thin-sections (generally six, at regular 30° strike intervals) plus horizontal thin-sections were cut from all samples. The strike, or pitch, of all relatively straight inclusion trail segments were measured on all sections, yielding a total of 7531 measurements. Following the procedure described in Aerden (2003), data were divided into two main categories: (1) orientations of straight to moderately sigmoidal inclusion trails, further called A-type microstructures, and (2) orientations of the axial traces of microfolded inclusion trails plus truncation lines associated with more complex inclusion trail patterns (B-type microstructures; Fig. 2a). Only sample 2 (eclogite) did not yield useful data due to the coarse size of inclusion trails and their smooth curvature. However, the rotation axes of these microstructures could be accurately measured using an alternative technique described in Section 4.2.

Rose diagrams for individual thin-sections generally exhibit single, bimodal, or trimodal preferred orientations of inclusion trails. Due to page limitations, only the rose diagrams for horizontal sections are reproduced in this article (Fig. 3a), whereas the rest of the data can be viewed as an electronic supplement to Aerden (2003) accessible via this Journal's Internet page. The combined data from differently oriented thin-sections of single samples were analysed further with the 'FitPitch' computer program

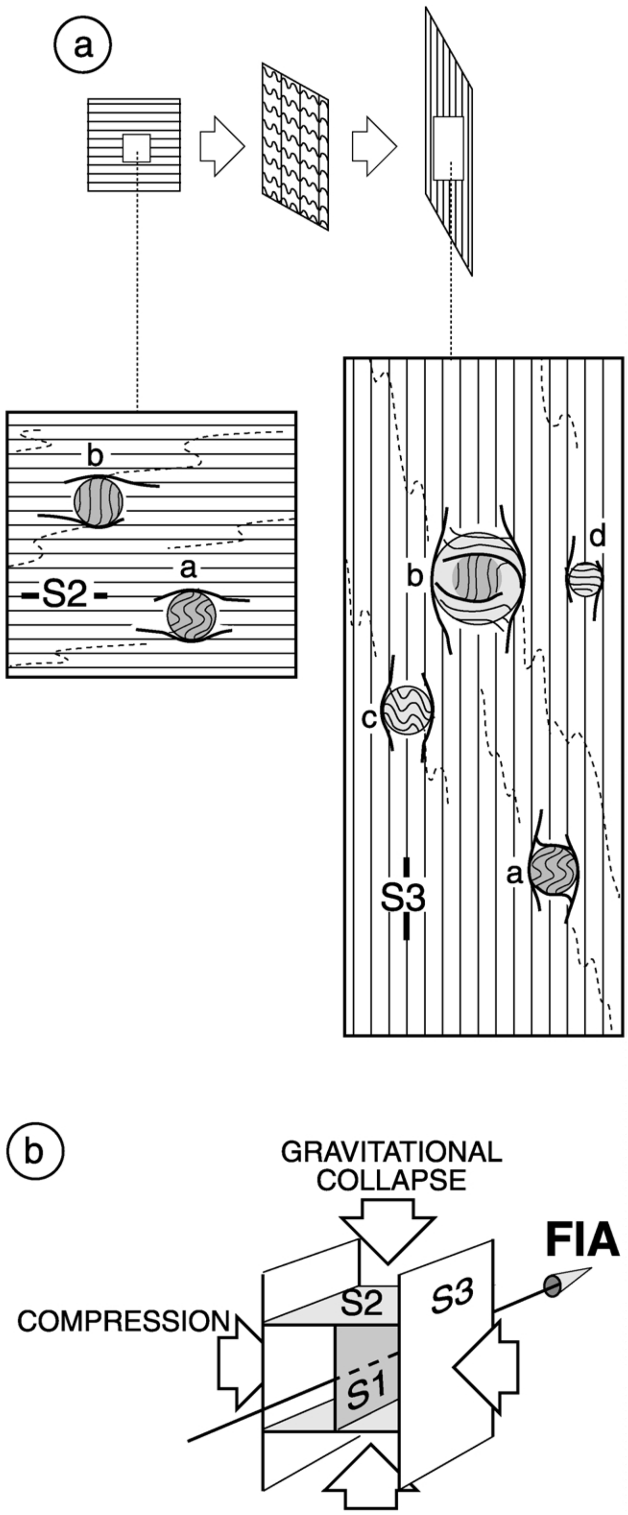

Fig. 2. (a) Conceptual model of progressive porphyroblast growth preserving successive orthogonal foliations. The effect of a hypothetical 'D_3' event is shown. Porphyroblasts *a* and *b* nucleated during D_2 and include S_1. During D_3, porphyroblast *a* does not grow, *b* has further growth, and *c* and *d* nucleate and enclose S_2. In terms of this study, the microstructures to be measured would be the straight trails in the cores of *b* and *d* (A-type microstructures), the axial trace of the crenulated trails in *a* and *c*, and the core-rim truncation in *b* (B-type microstructures). (b) Sketch of spatial relationship between FIA, foliation orientations and inferred direction of bulk crustal shortening.

(Aerden, 2003). This program allows calculation of up to three planes of preferred orientation of inclusion trails, irrespective of whether these represent a single foliation or multiple foliations. Data are fitted to either one, two or three best-fit planes, purely based on which of these options yields the smallest normalised standard deviation. Graphical representations of results for all samples are given in the above-mentioned electronic supplement, while here I will only emphasise a general result concerning the entire sample collection. Namely, the computer analysis reveals that this data contains a moderate preference of best-fit planes for steeply dipping or subhorizontal orientations (Fig. 4a and b). A similar pattern is actually also present in the raw (2-D) data, although it is quite weak for A-type microstructures (Fig. 4c and d). Its significance will be discussed later.

4.2. Foliation intersection axes (FIA)

The curvature axes of sigmoidal and spiral-shaped inclusion trails, termed foliation intersection- or inflexion axes ('FIA'; Bell et al., 1995) were determined using the method first described by Hayward (1990). This method uses multiple thin sections cut in a radial pattern through a sample, and requires that a large majority of inclusion trails exhibit consistent curvature senses in single thin-sections (S or Z asymmetry). The FIA trend can then be located between the strikes of two vertical thin-sections that record a switch in the dominant curvature asymmetry. Only eight of all thirty analysed samples proved suitable for this technique (Fig. 3a), as the rest contain mainly straight inclusion trails, symmetrically crenulated inclusion trails, or sigmoidal inclusion trails with highly inconsistent curvature asymmetries in single thin-sections. Inclusion trail curvature reversals from the core to the rim of single porphyroblasts (Bell et al., 1995) were too scarce in any of the samples to reliably determine multiple FIA potentially preserved in some samples. FIA plunges were not determined using the FIA method as this would have required a still larger number of thin-sections, and because the computer analysis yields the plunge of best-fit FIA (Fig. 4b). Intersection-lineations and crenulation axes in the matrix can be considered equivalent microstructures to FIA and are called 'matrix FIA'. In some samples, 'matrix FIA' are continuous with and parallel to FIA within the porphyroblasts (e.g. samples 8 or 16; Fig. 3a). In others, both are defined by different foliations with unrelated orientations (e.g. samples 2 or 15; Fig. 3a).

5. Qualitative microstructural analysis

5.1. Coaxial foliation sets

Microstructural analysis was greatly enhanced by line tracings of porphyroblasts, which were compiled on microstructural maps for individual thin-sections. These maps show that bimodal or trimodal inclusion trail orientations (Fig. 3a) generally correspond to multiple foliations preserved within progressive growth zones of single porphyroblasts and/or within mixed groups of porphyroblasts of different age (and sometimes different mineral composition (Figs. 5a–d, 6a and c, 7 and 8a). Correlations established further in this paper indicate the existence of four sets of inclusion trails with distinctive, regionally consistent strikes, and consistent relative timing. Vertical sections and field data reveal further that each set comprises multiple foliations with a common strike, although they are not necessarily all developed in a sample. These four sets of coaxial foliations, which will be labelled FS_1–FS_4 (i.e. foliation set), are associated with four sets of FIA (FIA_1–FIA_4). The subhorizontal attitude of these FIA is independently indicated by the FitPitch analysis (Fig. 4b).

5.2. A closer look at samples 3–6

Samples 3–6 were taken from a single outcrop in the Ordenes Complex (Fig. 1) where deep levels of the Basal Unit are exposed, as demonstrated by Arenas et al. (1995), from the composition of mineral inclusions in albite and garnet porphyroblasts. These authors did not focus on the detailed geometry of inclusion trails, which they assumed represented a single fabric (their 'S_1'). However, microstructural observations described here reveal a polyphase origin, which is given particular attention because of the potential implications for the kinematics of early-Variscan subduction stages in NW-Iberia (see Section 9), and to illustrate the concept of foliation sets.

The samples in question contain abundant albite porphyroblasts whose inclusion trails have a bimodal distribution of strikes (Fig. 3a). Overprinting relationships in horizontal sections indicate a younger age of NNE–SSW striking inclusion trails with respect to older E–W-trending trails (Figs. 6c and 8d). In vertical sections, evidence for a more complex fabric succession is observed. Some albite porphyroblasts enclose older garnet porphyroblasts whose inclusion trails are generally moderately to steeply dipping (Fig. 8a). This early fabric is called S_1 in this section. It is overprinted by a subhorizontal crenulation cleavage (S_2) preserved in a first group of albite porphyroblasts, which is in turn overprinted by a subvertical crenulation cleavage (S_3) preserved in a younger group of albite porphyroblasts. S_3 is continuous with, but oblique to, the principal matrix schistosity, which is still overprinted by a coarsely spaced crenulation cleavage (S_4; Figs. 7 and 8a). Alternative interpretation of S_3 /S_4 as an S–C fabric is considered unlikely due to the following points: (i) the orthogonal relationship between S_2, S_3 and S_4 (Fig. 8b), (ii) isoclinal folds of S_3 with S_4 parallel to the axial plane, and (iii) a period of porphyroblast growth that separates both foliations in time. The main matrix foliations (S_3 and S_4) are still regionally folded with upright, NNE–SSW striking axial planes, locally associated with a penetrative crenulation cleavage (S_5).

Thus, three internal foliations (S_1–S_3) overlapping with three matrix foliations (S_3–S_5) have been described so far. However, an even more protracted deformation history is indicated by some larger garnet crystals whose staircase- or spiral-shaped inclusion trails probably represent a succession of suborthogonal foliations (cf. Bell and Johnson, 1989; Stallard and Hickey, 2001), two of which predate S_1 (S_0 and S_{-1}; Fig. 8c). The scarcity of such garnets prevented determination of their FIA, but abundant garnets with very similar inclusion trail patterns occur at a different outcrop 15 km to the north (sample 2) and yield an E–W FIA trend. This is subparallel to the strike maximum of the older inclusion trail at the outcrop considered here.

In summary, a succession of up to seven suborthogonal foliations appear to be preserved in progressive porphyroblast growth stages and in the matrix, which define two foliation sets: an older E–W striking set (S_{-1}–S_1), and a younger NNE–SSW striking set (S_2–S_5). Considering the orientation data from other sample locations in the Basal Unit (see next section), some isolated microstructures (Fig. 8d) at the outcrop discussed here could possibly belong to a third foliation set (FS_2) with intermediate timing, but greatly underrepresented with respect to FS_1 and FS_3.

6. Microstructural correlation

The orientations of the main matrix foliation, main mineral lineation, matrix-FIA, porphyroblast-FIA, B-type- and A-type inclusion trails in all samples are shown in Fig. 3a. Matrix FIAs are consistently younger or of the same age as porphyroblast FIA or B-type microstructures, and the latter are consistently younger or of the same age as A-type microstructures. Thus, microstructural ages increase from left to right in Fig. 3a. Overprinting relationships described in preceding sections establish the relative age of multiple generations of A-type or B-type microstructures associated with bimodal or trimodal rose diagrams. In order to correlate the fabrics of different samples, three subareas will be considered where mapped fabrics and structures provide a common reference frame for microstructural timing.

The first subarea comprises samples from the Basal Unit and para-autochthonous unit in the Ordenes- and Malpica-Tuy complexes (samples 1–14), plus the one Upper Unit sample (sample 15). Inclusion trails with high-pressure mineralogy in these samples define an early E–W-trending set of foliations (FS_1), which is overprinted by NNW–SSE (sample 1, samples 11 to 14) and NE–SW-trending foliations (samples 2–10). The relative timing of the younger trends is indicated by overprinting relationships preserved in samples 9 and 10 (Figs. 5c and 8d). Thus, the microstructural development in this subarea can be inferred to comprise three foliation sets labelled FS_1–FS_3. The

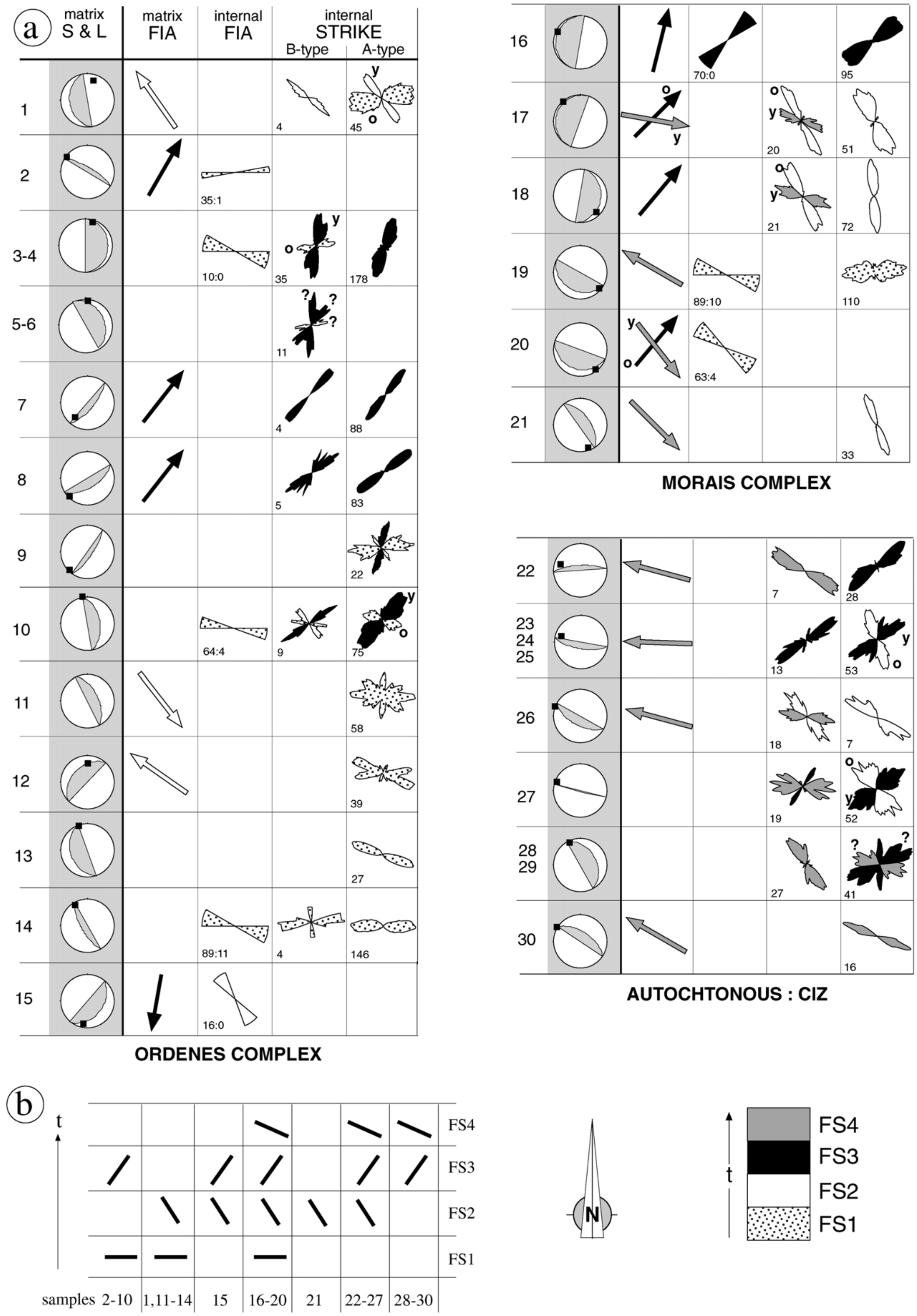
a
matrix S & L
matrix FIA
internal FIA
internal STRIKE
B-type
A-type
ORDENES COMPLEX
MORAIS COMPLEX
AUTOCHTONOUS : CIZ
b
t
FS4
FS3
FS2
FS1
samples 2-10 1,11-14 15 16-20 21 22-27 28-30
N
FS4
FS3
FS2
FS1

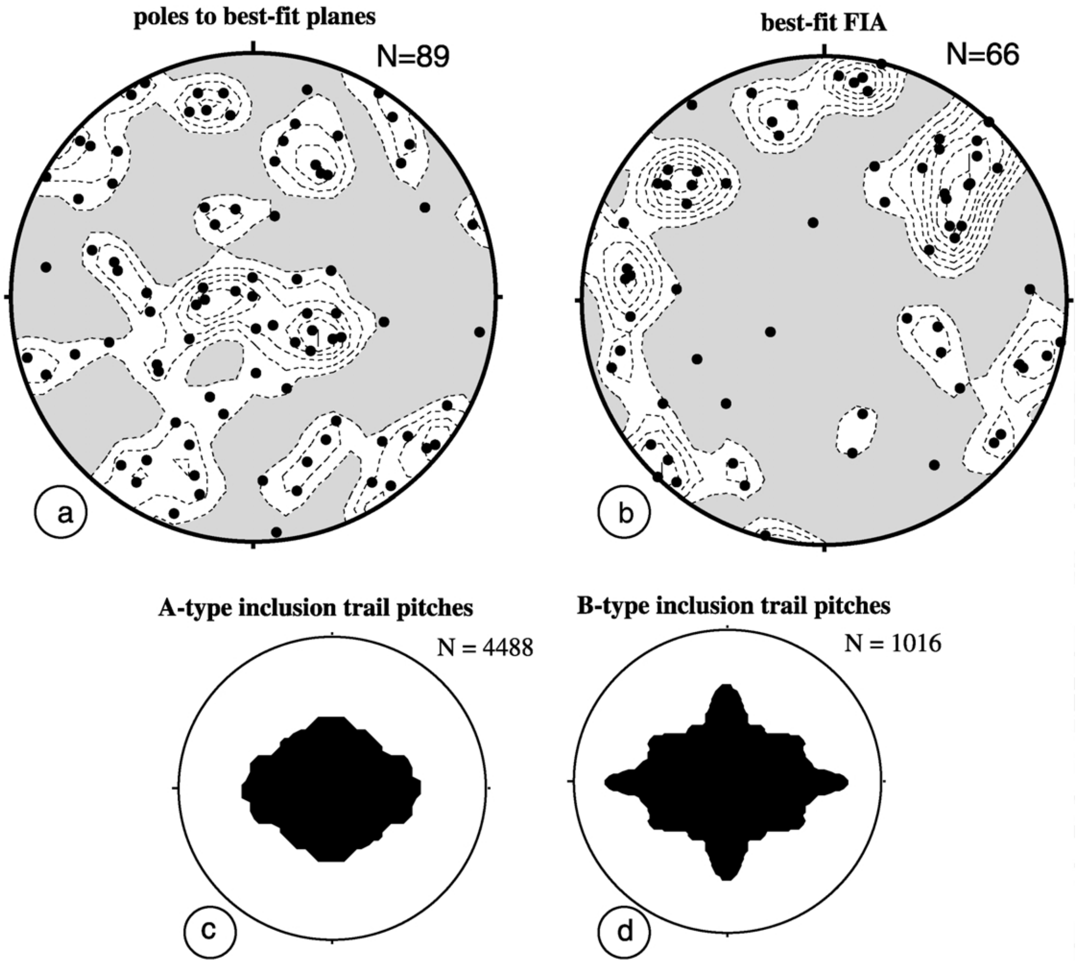

Fig. 4. (a) Poles to calculated best-fit planes for inclusion trail surfaces in each sample. Note that poles are preferentially located near the centre and the perimeter of the plot. Contours are multiples of a uniform distribution. (b) Intersection-lines between (multiple) best-fit planes calculated for individual samples or 'best-fit FIA'. These have mainly gentle plunges. (c) Moving average rose-diagram (10° counting interval) for pitch angles of A-type inclusion trails in all samples measured on a total of 96 vertical thin sections with variable strikes. Weak vertical and horizontal preferred orientation can be noticed. (d) As above for B-type inclusion trails, which show stronger orthogonal preferred orientations (see Section 9.1 for discussion).

sample from the Upper Unit contains the same matrix FIA as samples 7 and 8, all defined by late crenulation axes (FS_3) associated with macroscopic NNE–SSW- to NE–SW-trending folds in the Ordenes Complex (Van Zuuren, 1969). Consequently, the NNW–SSE striking inclusion trails in this sample can be tentatively correlated with FS_2 in the Basal Unit.

The second subarea was partially mapped by this author (see Section 7.2) and comprises samples from both the Basal Unit of the Morais Complex (samples 16–27) and from its immediate footwall (Central Iberian Zone). The dominant matrix foliation in these samples has been regionally folded and overprinted by different generations of crenulation cleavages related to FS_3 and FS_4 (Fig. 3a). Older inclusion trail generations mainly have NNW–SSE trends (FS_2) and are generally discontinuous with the matrix fabrics (Fig. 5a and b). Microstructural trends and their overprinting relationships in this subarea suggest three foliation sets (FS_2–FS_3–FS_4; Fig. 3a). The existence of an older foliation set (FS_1) in samples 19 and 20 has been inferred from the similar composition and strike of very fine-grained, graphitic inclusion trails in these samples and in samples 12–14 of subarea 1.

The third subarea (samples 28–30) is situated in the

Fig. 3. (a) Chart showing in four columns from left to right: (1) orientation of main matrix foliation (S; equal-area plot) and stretching lineation (L; black squares), (2) the trend of matrix FIA, (3) the trend range of porphyroblast FIA, (4) the strike of A-type, and (5) B-type inclusion trails. The latter are plotted in moving-average rose diagrams constructed with 'Stereoplot' (N. Mancktelow) using a 20° counting interval. The number of data is indicated on the figure. Numbers below FIA data indicate numbers of inclusion trails with consistent versus inconsistent curvature sense in a sample (see Section 4.2). Where known, the age relationship between different orientation maxima for the same type of microstructure is indicated with 'y' (younger) and 'o' (older). Note the independence between dominant structural trends in the matrix (S and L) versus the orientation of inclusion trails. (b) Summary of age relationships between different microstructural trends in the separate subareas discussed in Section 6.

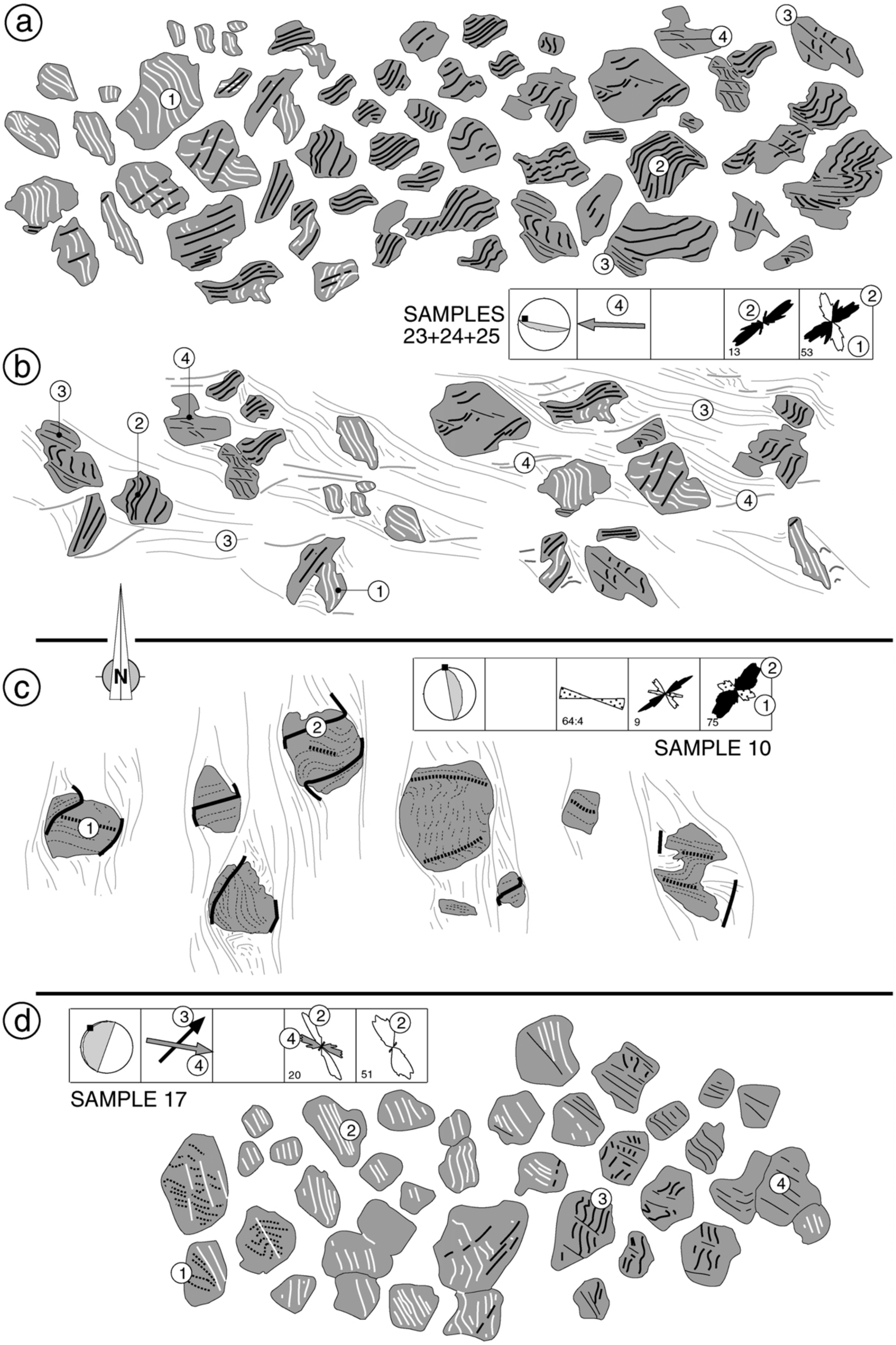
a
SAMPLES
23+24+25
b
c
SAMPLE 10
64:4
d
SAMPLE 17

Central Iberian Zone south-west of Salamanca (Fig. 1). Cordierite porphyroblasts in sample 30 grew in the contact aureole of a late-orogenic granite, and include a subvertical finely spaced crenulation cleavage (FS_4), which is continuous with, but oblique to, a moderately dipping matrix schistosity. Regional mapping by Díez Balda et al. (1995) showed that towards lower structural levels, this matrix schistosity is progressively rotated and transposed in a wide subhorizontal shear zone that formed during synorogenic gravitational collapse. Samples 28 and 29 (staurolite–andalusite–garnet schist) are located within this shear zone. Their B-type inclusion trails are parallel and continuous with the principle shear zone foliation (S_2 of Díez Balda et al., 1995), whereas older A-type inclusion trails preserve occasional (due to intense chemical alteration) mutual overprinting relationships and have more scattered orientations that are interpreted as a mixed FS_3–FS_4 population (Fig. 3a).

A comparison of the data from the three subareas reveals a consistent pattern of four superposed microstructural trends (Fig. 3b), which is better appreciated after placing the data in a chronological order (Fig. 9a). In the next section, we will investigate the significance of this pattern and its possible correlation with successive generations of fold axes and mineral lineations recognised in the field.

7. Correlation with field structures

7.1. Cabo-Ortegal and Ordenes Complexes (subarea 1)

Early studies in the Cabo-Ortegal Complex and the south-west corner of the Ordenes Complex documented six folding phases (Van Zuuren, 1969; Engels, 1972), although the relative timing of the earlier folding phases was uncertain. Two principal sets of fold axes (and subparallel mineral lineations) were distinguished: an early set associated with isoclinal folds or so-called 'syn-schistosity folds' ($F_{1,2,3}$ of van Zuuren plus $F_{1,2}$ of Engels), and a younger set associated with crenulation cleavages ($F_{4,5,6}$ of van Zuuren plus $F_{3,4,5}$ of Engels). The younger lineations and fold axes show consistent NE–SW to N–S trends parallel to macroscopic regional folds and produce matrix FIA_3 in samples 7, 8 and 15 (Fig. 3a). The older group of lineations and fold axes correspond to local low strain domains (fold hinges, boudins, etc.) and exhibits trends similar to FS_1 and FS_2 microstructures recognised in this study (Fig. 10). Thus, fold axes and lineations described by Van Zuuren and Engels mimic the orientation of three microstructural trends preserved within porphyroblasts (Fig. 9b and c). The only anomaly is the relative timing of a N–S-trending L_1 of Van Zuuren (1969), which would imply pre-FS_1 deformation that has not been detected in this study. However, Van Zuuren (1969) based his timing merely on the scarcity of F_1 fold trends in his study area, compared with more common E–W-trending syn-schistosity folds (F_3 and F_2). Overprinting relationships reported by Van Zuuren only constrain the timing of L_1 to pre-F_4, so it may in fact be syn-FS_3 (Fig. 9c). Open, late-Variscan folds in the Cabo-Ortegal and Ordenes complexes with WNW–ESE trends postdate all of the fold generations described above and are partially responsible for the basinal geometry of both complexes (e.g. Martínez Catalán et al., 1996). Their post-FS_3 timing and trend allows them to be correlated with more intensely developed FS_4-related structures further south, which are described in the next section.

7.2. Morais Complex and Central Iberian Zone (subarea 2)

The basal thrust of the Morais Complex and para-autochthonous unit or 'Main Tras-os-Montes Thrust' (Ribeiro et al., 1990) as well as other tectonic contacts higher in the nappe stack are associated with a gently to moderately dipping crenulation cleavage ('S_2' of Ribeiro, 1974), asymmetric folds with sheared limbs, and millimetre- to metre-scale shear bands developed under greenschist facies conditions. These structures deform a regional schistosity ('S_1' of Ribeiro, 1974), but are themselves weakly to moderately overprinted by late WNW–ESE- to NW–SE-trending folds associated with a subvertical crenulation cleavage ('S_3' of Ribeiro, 1974). Structural mapping by the author in the Morais Complex and its autochthonous footwall has provided evidence for two additional folding phases with intermediate timing between 'S_1' and 'S_2' of Ribeiro (1974). These are referred to as F_x and F_y folds, respectively, in order to maintain the original S_1–S_2–S_3 terminology of Ribeiro (1974).

In the footwall units of the Main Tras-os-Montes thrust (Central Iberian Zone), the D_2 deformation is generally weak, except in zones closely bordering the Main Tras-os-Montes Thrust and another, newly recognised thrust (Fig. 11a). Mapping of the regional schistosity (S_1) revealed a dome-and-basin structure cut by (and hence pre-dating) the Main Tras-os-Montes Thrust. The domes and basins developed from interference between early NE–SW-trending upright folds (F_x) and younger WNW–ESE-trending

Fig. 5. (a) Line drawings of porphyroblasts in horizontal sections of samples 23–26. Numbers in circles indicate the relative timing of different inclusion-trail generations. Corresponding data in Fig. 3a have been inserted to indicate their relationship with different microstructural age sets. (b) Relationships between inclusion trails and matrix foliations in the same samples as (a). The fourth foliation (4) included in a few porphyroblasts is a widely spaced external crenulation cleavage that cuts the thin-section at a low angle (S_2 in Section 7.2). (c) Line drawings of representative porphyroblasts in horizontal sections of sample 10. NE–SW striking inclusion trails overprint E–W to NW–SE striking trails. Corresponding data from Fig. 3a have been inserted to indicate their relationship with different microstructural age sets. (d) Line drawings of porphyroblasts in horizontal sections of sample 17. Quantitative orientation data for this sample from Fig. 3a have been inserted.

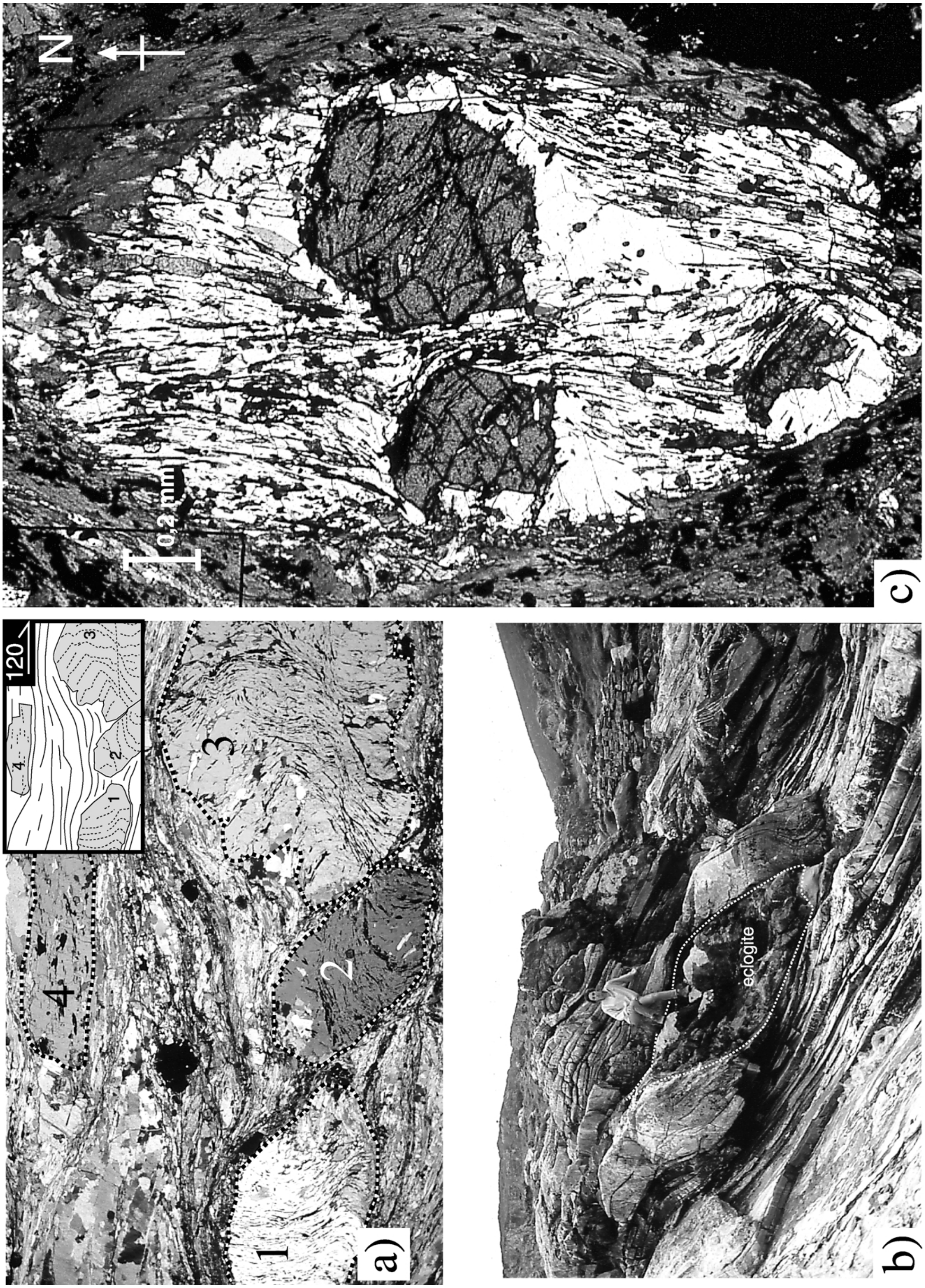
N
0.2 mm
c)
120
1
2
3
4
a)
eclogite
b)

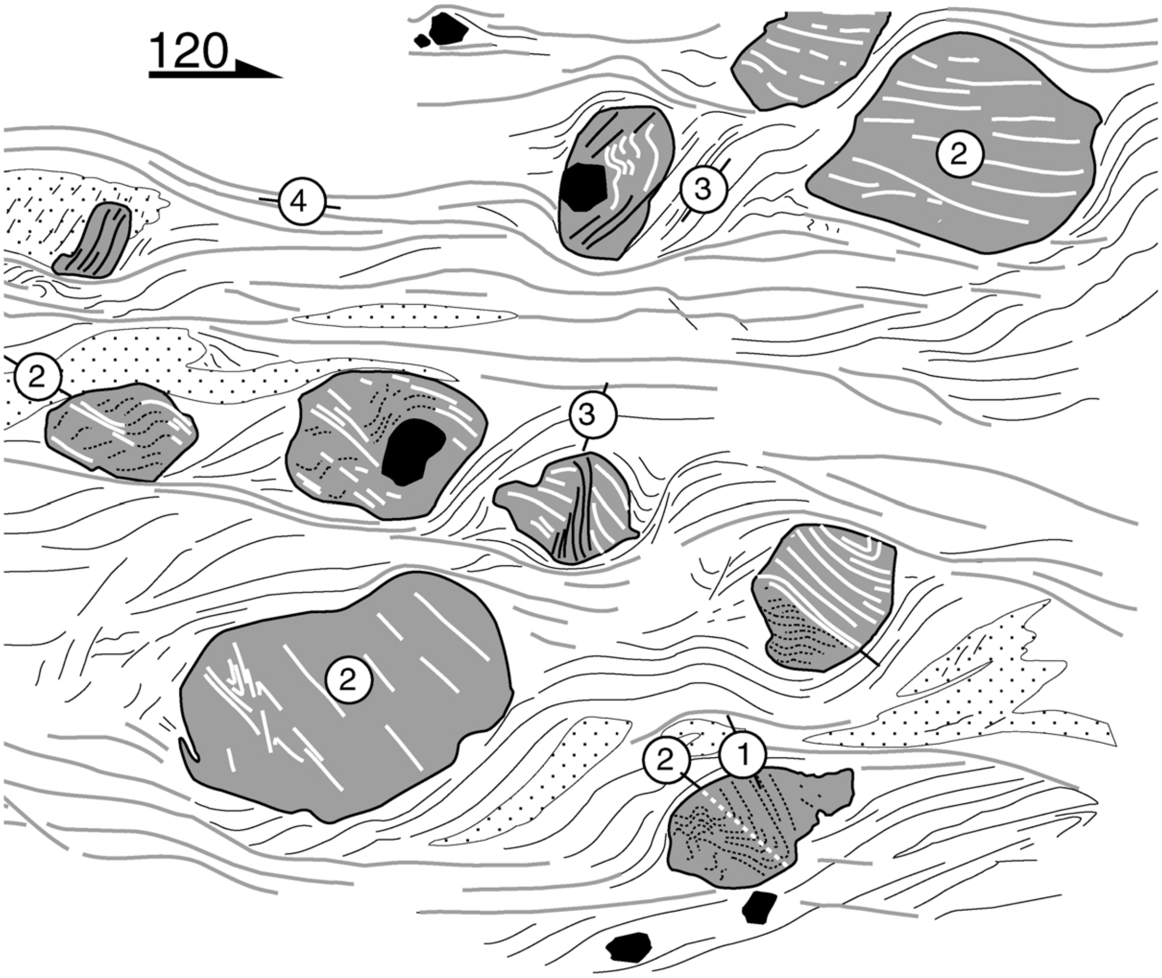

Fig. 7. Line diagram of a vertical thin-section of sample 5. Microstructural relationships document a succession of four foliations with consistent orientations (S_1–S_4). Without information from inclusion trails, a single phase of shearing could be erroneously concluded by interpreting S_3 and S_4 as an S–C fabric.

upright folds (F_y) with similar orientations as F_3 folds, but predating S_2 (Figs. 9e and 11a).

In the hanging wall of the Main Tras-os-Montes Thrust (para-autochthonous and allochthonous units) evidence for pre-nappe (pre-S_2) folding and crenulation of S_1 about F_x and F_y axes was observed at different outcrops and in thin-sections. A regional map of S_1 (Fig. 11a) also indicates folding of S_1 prior to D_2, even though no regular F_x–F_y fold-interference pattern is observed, probably due to much more penetrative D_2 strain. The latter caused vertical flattening and rotation of all pre-F_2 structures to low dip angles, after which these structures were still folded by F_3. Nevertheless, regional-scale F_x and F_y fold trends are still well manifested on a structural map of L_2 (intersection-lineations between S_1 and S_2 and related fold axes; Fig. 11b). The reason is that S_2 developed in a subhorizontal orientation, so that its intersection with S_1 coincides with the original strike of S_1, presumably controlled by F_x and F_y folds. In effect, L_2 exhibits a pattern of predominant NE–SW trends (F_x) overprinted by WNW–ESE trends (F_y) in narrow corridors.

Crenulation cleavages associated with F_x, F_y, F_2 and F_3 produce the FS_3- and FS_4-related microstructures in subarea 2 (Figs. 3a and 5a and b), whereas older inclusion trails mainly have NNW–SSE trends (FS_2) and are discontinuous with the matrix foliations. Similar pre-S_1 inclusion trails of garnet porphyroblasts in the lower and higher-grade structural levels of the autochthonous unit record maximum pressures of about 900 MPa (Escuder Viruete et al. 1994; their "S_1").

Fig. 6. (a) Photomicrograph of four albite porphyroblasts in a vertical section of sample 3 from the Basal Unit at Ordenes. The lower three preserve microfolded trails with parallel axial traces. The elongate upper porphyroblast grew after transposition of the foliation preserved in the other porphyroblasts (compare with Fig. 2a). (b) Outcrop of sample 2 (eclogite) showing large eclogite boudin surrounded by strongly deformed paragneisses of the Basal Unit. (c) Albite porphyroblast in sample 3 with NNE–SSW striking crenulation cleavage. This post-dates WNW–ESE striking inclusion trails in older garnet (see line diagram in top-left corner of Fig. 8d). Both orientations are seen in the corresponding rose diagram in Fig. 3a.

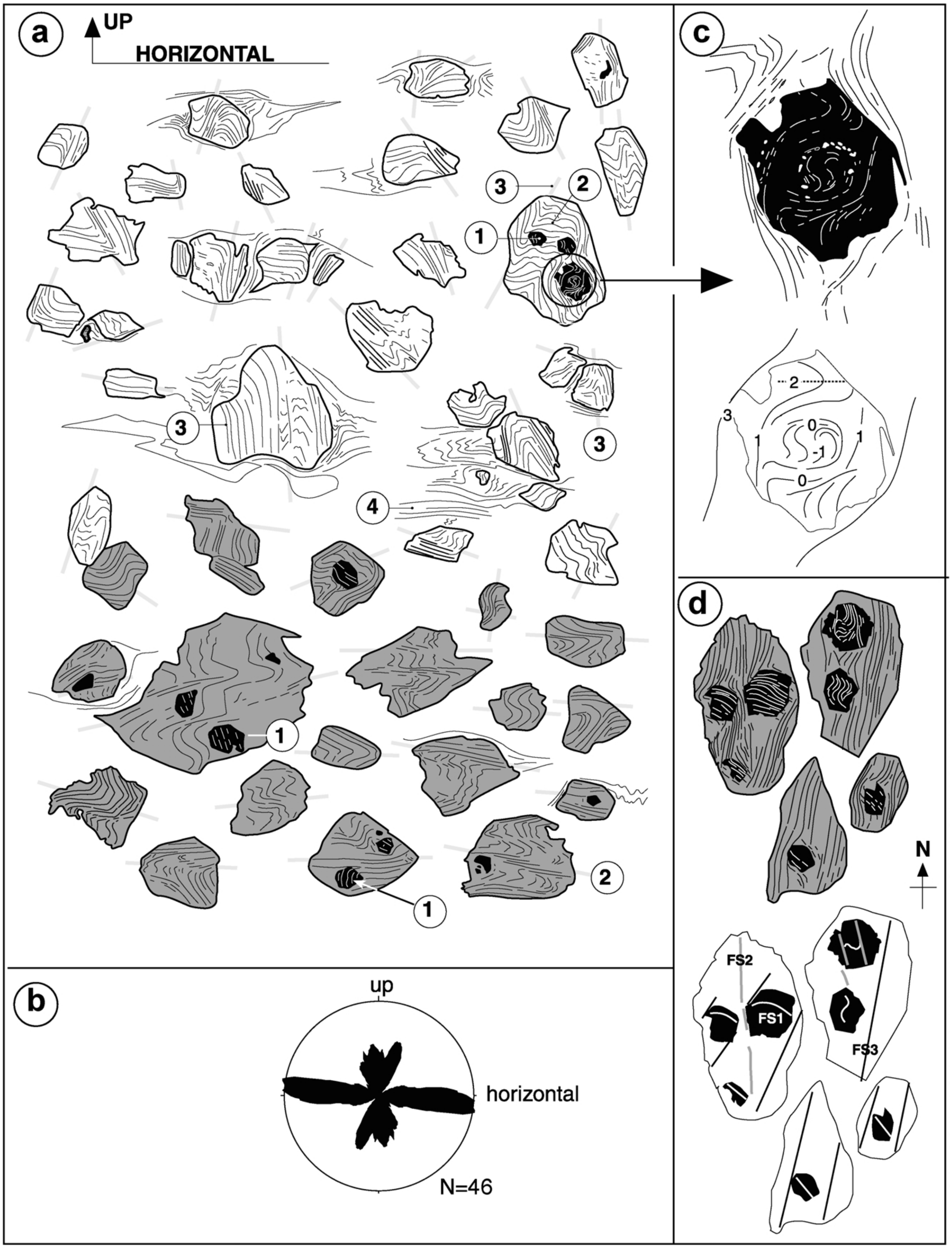
a
UP
HORIZONTAL
1
2
3
4
b
up
horizontal
N=46
c
2
3
1
0
-1
d
N
FS2
FS1
FS3

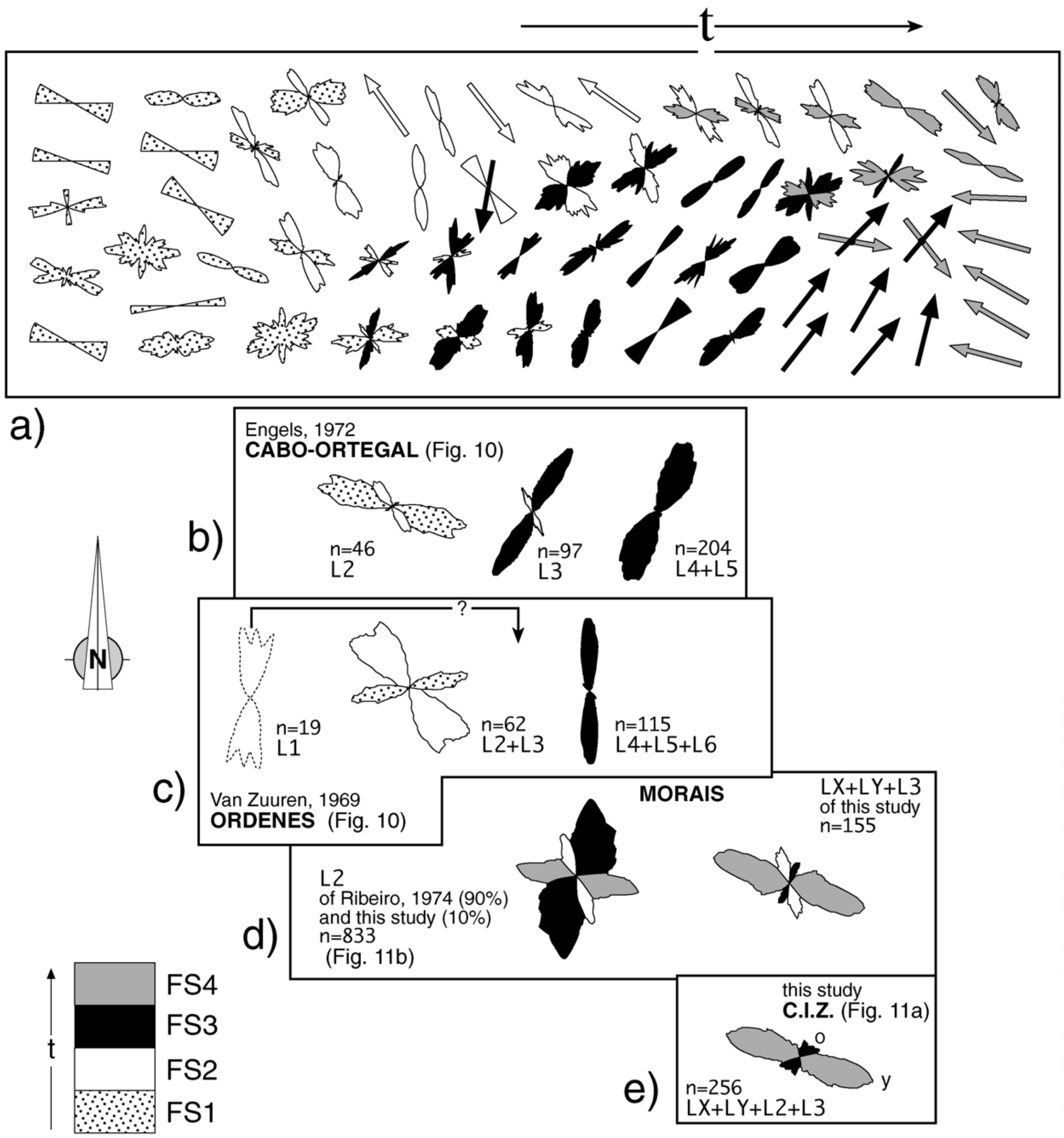

Fig. 9. (a) Microstructural data from Fig. 3a placed in chronological order based on relative timing evidence. (b)–(d) Trends of different generation fold and crenulation axes measured by different workers in the Cabo-Ortegal, Ordenes and Morais allochthonous complexes. (e) Trends of different generation fold and crenulation axes measured by different workers in the Central Iberian Zone south-east of Morais (autochthonous of subarea 2 in main text). See Sections 7.1 and 7.2 for detailed description and interpretation.

Thus, the post-main cleavage evolution of autochthonous and allochthonous units appears to have been essentially the same, except for much larger D_2 strain in the latter. Five foliation generations (S_1, S_2, S_x, S_y, S_3) can be recognised in both domains and grouped in two foliation sets: NE–SW trending FS_3 (S_1, S_x) and WNW–ESE trending FS_4 (S_y, S_2, S_3). Both foliation sets developed during the exhumation of allochthonous and autochthonous units, although the main

Fig. 8. (a) Line drawings of porphyroblasts with B-type microstructures in different vertical sections of samples 3 and 4. The main matrix schistosity in the samples (S_3) dips gently and transposes S_2, which in turn transposes S_1 included in small garnet crystals. (b) Moving-average rose diagram (20° counting interval) for the orientation of internal crenulations in (a) reflecting orthogonal relationship between S_2 and S_3. (c) Garnet porphyroblast containing spiral inclusion trails with two pre-S_1 foliations showing truncational relationships. (d) Porphyroblasts in horizontal sections recording FS_1, FS_2 and FS_3 trends, although FS_2 is statistically underrepresented. A photomicrograph of one of these porphyroblasts is given in Fig. 6c.

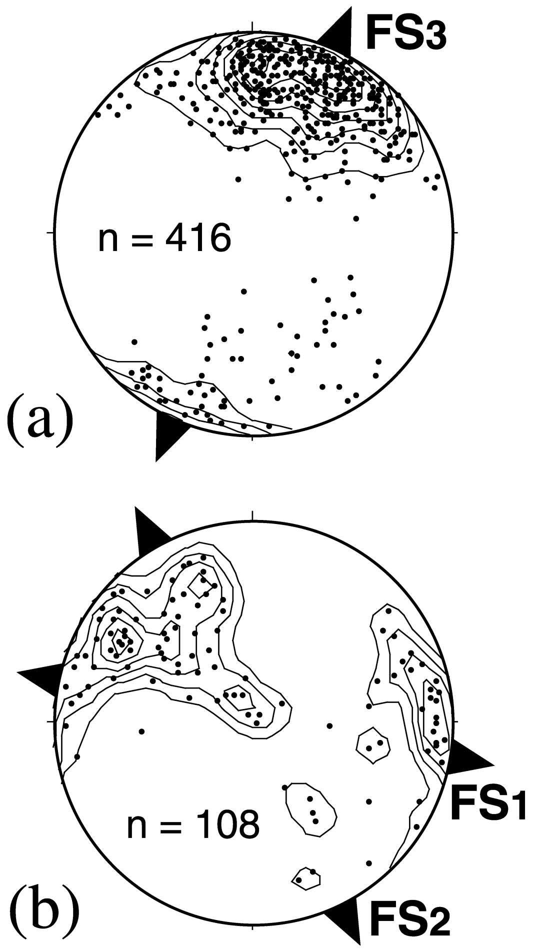

Fig. 10. Lineation measurements of Van Zuuren (1969) and Engels (1972) in their respective study areas indicated in Fig. 1. Post-schistosity lineations ($L_4 + L_5 + L_6$ of Van Zuuren plus $L_3 + L_4 + L_5$ of Engels) trend parallel to regional-scale folds and FS_3 of this study. Older syn-schistosity lineations ($L_2 + L_3$ of Van Zuuren plus L_2 of Engels) match the trends of FS_2 and FS_1. The timing of L_1, as proposed by Van Zuuren, is reconsidered in this paper (see Section 7.1 and Fig. 9c).

regional foliation (S_1) is a composite fabric as witnessed by scarce intrafolial fold relicts observed in the field and pre- to syn-S_1 inclusion trails (FS_2 and FS_1). The Main-Tras-os-Montes thrust is a relatively late brittle-ductile structures (D_2) that transported already exhumed allochthonous rocks horizontally under greenschist-facies conditions.

8. Absolute timing of deformation

Existing geochronological data only provide imprecise constraints on the absolute timing of successive foliation sets distinguished in this paper:

1. Prominent NE–SW-trending folds in the Ordenes and Cabo-Ortegal Massifs (late syn-FS_3) also affect the Central Iberian Zone and Western Asturo-Leonese Zone further east. In the last-mentioned zone, ages between 320 and 310 Ma have been reported for these structures by Dallmeyer et al. (1997).
2. A late and continuous tectonic contact situated near the base of the Ordenes Complex (‘Pico-Sacro Detachment’; Fig. 1) cuts a previously folded regional foliation and a granite body dated at 323 ± 11 Ma (Martínez Catalán et al., 1996). The ‘Main Tras-os-Montes Thrust’ at Morais (correlated as FS_4) shows identical cross-cutting relationship with respect to a folded footwall foliation, a very similar map geometry, and is most probably of the same age.
3. The regional foliation in samples 22–27 of the Central Iberian Zone (S_1 in the preceding section) developed partially during exhumation of these rocks. Attempts to date this foliation have provided disparate ages of 337 ± 2 (Galibert, 1984) and 326 ± 3 Ma (Escuder Viruete et al., 1998), respectively. The composite nature of S_1 (mixed FS_1-, FS_2- and possibly early FS_3 fabrics) makes it difficult to interpret these ages. 326 Ma should be the youngest possible age of FS_2 but it could be much older.
4. Ages for subduction-related high-pressure metamorphism in the Basal Unit of 374 Ma (Van Calsteren et al., 1979) and 365 Ma (Santos Zalduegui et al., 1995) should correspond to FS_1 microstructures, which are defined by HP minerals. The same minerals also define FS_2 and FS_3 in the basal unit, but this may indicate metastability during much of the exhumation history.

The above-described geochronological evidence suggests FS_1 plus FS_2 are between 365 and 330 Ma (Lower Carboniferous), while development of FS_4 ended after 310 Ma.

9. Interpretation and discussion

9.1. Kinematic significance of microstructural data

The results of this study must be considered in the light of two end-member models for the development of curved inclusion trails that envisage non-rotation versus rotation of porphyroblasts in a reference frame fixed to bulk kinematic axes (this reference frame is implied wherever the term ‘rotation’ is used further). According to the ‘non-rotation model’, sigmoidal and crenulated inclusion trails develop where porphyroblasts grow over a foliation that is undergoing progressive deformation and reorientation in a superposed strain field. The porphyroblasts do not rotate due to the partitioning of deformation into anastomosing zones of progressive shearing surrounding ellipsoidal domains of progressive shortening, or zero strain in the case of rigid objects (Bell, 1985). Consequently, FIA are

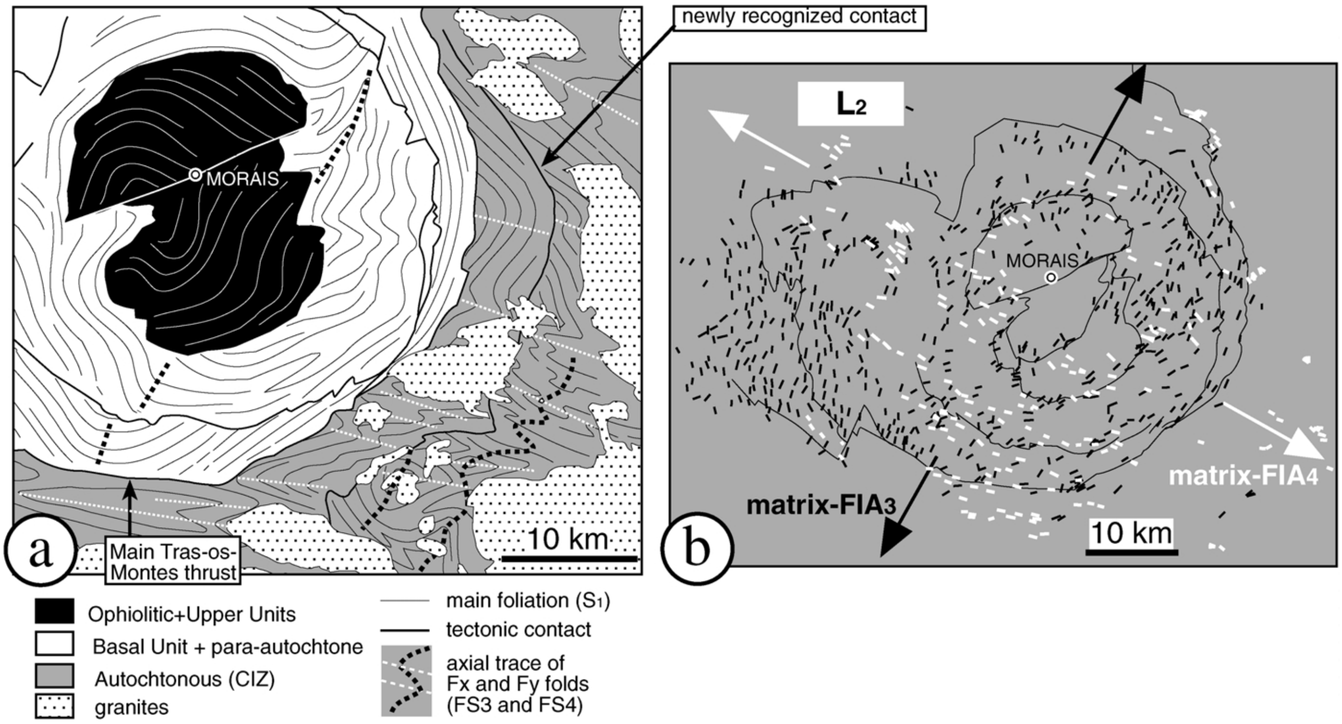

Fig. 11. (a) Form trace map of the main regional foliation in the Morais allochthon, and (para)autochthonous units. Folds (F_x and F_y in main text) are cut by younger nappe contacts. The same fold trends are apparent from micro- and mesocopic orientation data plotted in Fig. 9e. Also note the newly recognised nappe contact below the Main Tras-os-Montes Thrust. (b) Map of L_2 intersection-lineations and fold axes in the Morais Complex interpreted as a mixed population of matrix FIA_3 (marked white) and matrix FIA_4 (marked black), as also suggested by the rose diagram for this data shown in Fig. 9d. Predominant NE–SW trends appear overprinted by WNW–ESE trends and mimic superposed fold trends in the autochthonous domain shown in (a). See Section 7.2 for detailed description of this data. About 90% of the data is from Ribeiro (1974); the rest is from this author.

regarded as intersection lines between two foliation planes (Fig. 2a), and preferred vertical and horizontal inclusion trail orientations are attributed to a dynamic equilibrium between horizontal plate forces and gravity during orogenesis (Bell and Johnson, 1989; Hayward, 1992; Johnson, 1992, 1999; Aerden, 1994, 1998). The latter is plausible in the present study area, where repeated stages of syn-orogenic crustal extension have been documented independently (e.g. Escuder Viruete et al., 1994; Martínez Catalán et al., 1996; Díaz García et al., 1999). FIA associated with such orthogonal inclusion trails would develop perpendicular to the direction of crustal shortening (Fig. 2b), so multiple FIA sets in a region would potentially record a succession of different crustal shortening directions (Bell et al., 1995, 1999).

In contrast, the 'rotation model' (e.g. Williams and Jiang, 1999) envisages porphyroblast rotation being a function of factors such as the shape-anisotropy of porphyroblasts, the vorticity of deformation, or the dominant folding mechanism. Folding by bulk-coaxial shortening is actually not expected to produce much porphyroblast rotation due to partial balancing of flexural flow-induced rotations and fold-limb rotations (Aerden, 1995; Jiang, 2001). Thus, FIA can obtain an almost identical significance as in the non-rotation model (i.e. crenulation axes) depending on tectonic setting. Also, vertical/horizontal inclusion trail patterns can, in principle, be attributed to a series of relatively coaxial crustal deformations driven by tectonic forces and gravity. In shear zones, however, FIA are assumed to have formed by vorticity-induced porphyroblast rotation, and any pre-existing FIA should have become reoriented. Vertical/horizontal inclusion trail patterns are therefore not expected in shear zones, and multiple FIA sets with distinctive orientations would merely indicate relatively homogeneous strain throughout the shear zone, causing similar reorientation of preexisting FIA.

The existence of four sets of inclusion trails with distinctive strikes in NW-Iberia is, in principle, inconclusive as to which porphyroblast model is more correct. However, the 'rotation model' is more restrictive in the sense that it would imply a succession of either relatively coaxial strains or non-coaxial strains of similar magnitudes in every analysed sample. Moreover, only the former possibility (coaxial strains) would potentially explain orthogonal preferred orientations of the measured inclusion trails (Fig. 4a–d), but both possibilities are equally questionable considering: (1) the presence of major shear zones of different age throughout NW-Iberia associated with regional-scale strain gradients (see references cited in Section 7); (2) the mixed provenance of analysed samples from the strongly-deformed base of a high-grade nappe complex (e.g. Fig. 6b) and from its autochthonous footwall; and (3) the occurrence of orthogonal inclusion-trail patterns in other Variscan regions, including a major ductile shear

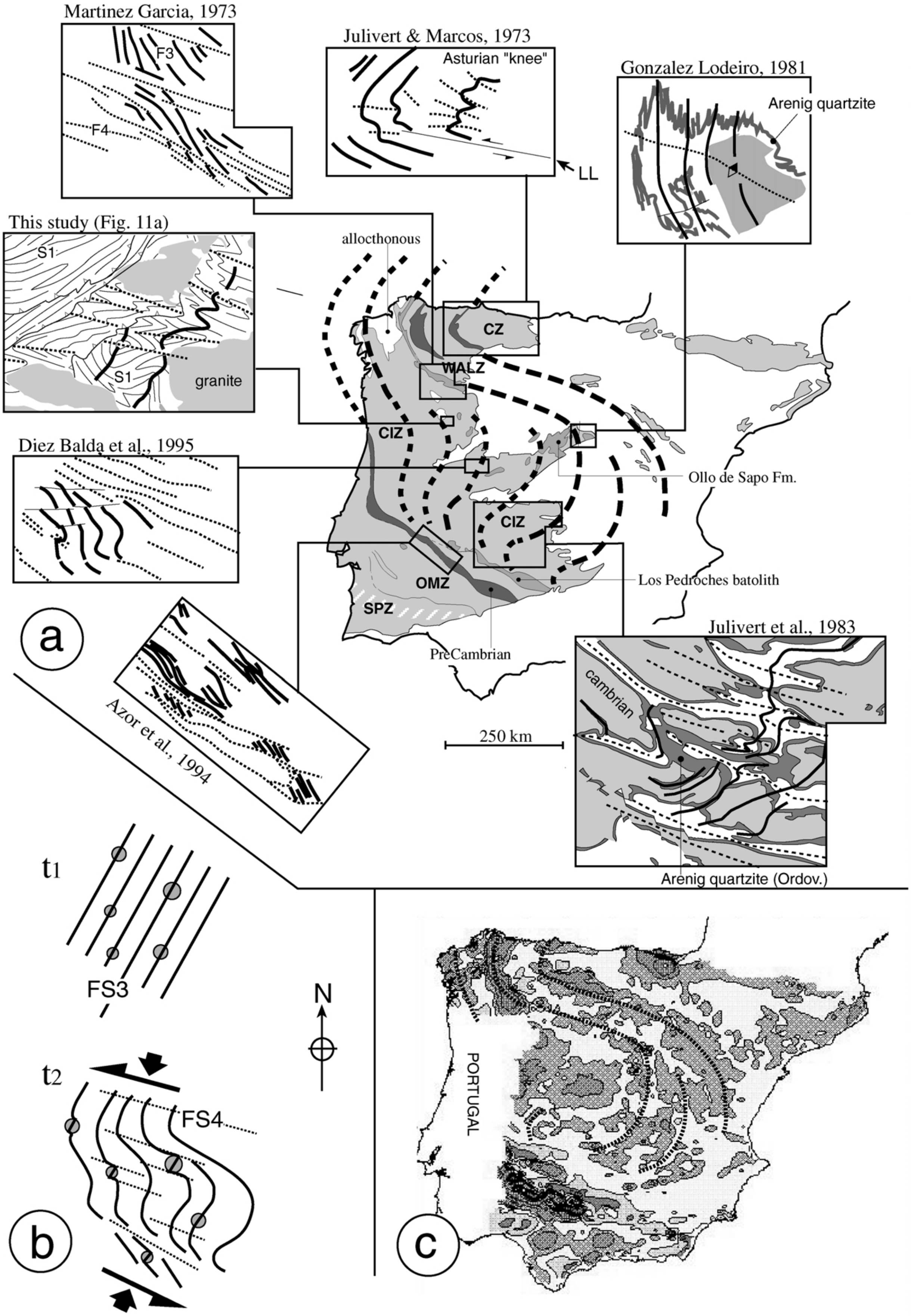

Martinez Garcia, 1973
F3
F4
Julivert & Marcos, 1973
Asturian "knee"
LL
Gonzalez Lodeiro, 1981
Arenig quartzite
This study (Fig. 11a)
S1
S1
granite
allocthonous
CZ
WALZ
CIZ
CIZ
OMZ
SPZ
Diez Balda et al., 1995
Ollo de Sapo Fm.
Los Pedroches batolith
PreCambrian
a
Azor et al., 1994
Julivert et al., 1983
cambrian
250 km
Arenig quartzite (Ordov.)
t1
FS3
t2
FS4
N
b
c
PORTUGAL

zone in the Montagne Noire (Aerden, 1994, 1998). All this rather suggests some microstructural mechanism that is capable of suppressing porphyroblast rotation during non-coaxial deformation. Geometric modelling of metamorphic microstructures (Bell, 1985) and some recent experimental studies (e.g. Takeda, 2001) suggest that this mechanism is closely related to self-organised partitioning of deformation in heterogeneous (polymineralic) media; a process that clearly requires more fundamental research. Limited vorticity-induced porphyroblast rotation is not excluded, and may have contributed to dispersing inclusion trail orientations in NW-Iberia. However, the spread in inclusion trail orientations may also reflect: (1) diachronous porphyroblast growth during progressive rotation of pre-existing foliations, (2) porphyroblast growth on opposite limbs of developing folds, or (3) late-stage rigid-body rotations induced by folding or faulting at high crustal levels (Aerden, 1995). In fact, processes (1) and (2) are consistent with the earlier observation that the orthogonal character of B-type microstructures is more pronounced than for A-type microstructures (compare Fig. 4c and d). The former represent incipient foliation development stages 'frozen' in porphyroblasts, whereas the latter represent more evolved and possibly reactivated foliations that presumably underwent larger amounts of reorientation before they became included.

In summary, the four sets of inclusion trails recognised in NW-Iberia are interpreted as a record of four periods of differently oriented crustal shortening, subperpendicular to the strike of these microstructures. For example, the E–W trend of FS_1 would relate to approximately N–S oriented subduction (in current geographic coordinates), which has actually also been inferred from conventional kinematic indicators (Burg et al., 1987; Ribeiro et al., 1990; Marques et al., 1992; Abalos, 1997). Each period of crustal shortening is inferred to have generated multiple foliations with a common strike due to second-order fluctuations in the balance between tectonic forces and gravity. The origin of apparently rapid (first-order) changes in the direction of crustal shortening is not known, but is expected to be related to changes in relative plate motion.

9.2. Implications for the Ibero-Armorican Arc

The Ibero-Armorican Arc is a major orocline in western Europe that connects the Iberian massif with the French Armorican Massif. In the study area, this orocline is outlined by the trends of macroscopic folds and thrusts that vary by approximately 90°. This curvature is reflected in the strikes of the dominant matrix foliations in the 30 analysed samples, but not in the strikes of their inclusion trails, which are independent of the location of a sample in the orocline (Fig. 3a). What implications does this have for the timing and mechanism of orocline development?

Previous workers have considered quite contrasting mechanisms of orocline formation, including (1) progressive indentation of a plate promontory (Matte, 1991; Dias and Ribeiro, 1995), (2) inheritance from a pre-Variscan curved plate boundary of similar shape as the present arc (Brun and Burg, 1982; Burg et al., 1987; Lefort and Agarwal, 1999), and (3) a late change in relative plate motion producing folding of an originally straight belt (Ries and Shackleton, 1976; Van der Voo et al., 1997; Weil et al., 2000). These models have been based on highly simplified regional-scale strain patterns and somewhat speculative structural correlations throughout the Ibero-Armorican Arc. Only the more strongly bent segment of the orocline in the Cantabrian Zone (Fig. 1) known as the 'Asturian knee' has been the subject of detailed structural and palaeomagnetic work aimed at unravelling the origin of this megastructure. Here, oroclinal bending is intimately related to large-scale cross-folding, which some workers have interpreted in terms of mechanism 3 (see above), namely, a change in crustal shortening direction from roughly E–W to N–S during the late-Carboniferous (Julivert and Marcos, 1973; Ries and Shackleton, 1976; Aller and Gallastegui, 1995; Weil et al., 2000). Others proposed that rotational thrust motions generated a thin-skinned orocline during a constantly directed plate collision (Julivert and Arboleya, 1984; Pérez Estaún et al., 1988), but this model conflicts with recent palaeomagnetic studies that have not found evidence for differential rotations between individual thrust sheets (Van der Voo et al., 1997; Weil et al., 2000). The porphyroblast data presented here not only support an origin of the Asturian knee in terms of a change in crustal shortening direction (mechanism 3 above), but further suggests that this model can be extrapolated to the entire Iberian Massif. In the northern part of the study area, the main macroscopic fold trends correlate with FS_3 and appear weakly overprinted by WNW–ESE-trending folds (Marcos, 2000; Fig. 12a). Further to the south, however, structural mapping by Martínez García (1973) and mapping of this study (Fig. 12a) demonstrate that FS_3-related fold trends are progressively overprinted and reoriented by WNW–ESE-trending folds and associated shear zones (FS_4). This may have resulted from large-scale sinistral transpression and associated heterogeneous reorientation and folding of an originally straight, N–S- to NE–SW-trending mountain

Fig. 12. (a) Fold interference patterns mapped in different parts of the Iberian Massif. NW–SE-trending folds (dashed lines) consistently overprint NE–SW- to N–S-trending folds (bold lines). The dashed lines in the study area of Azor et al. (1994) are low-grade sinistral faults associated with a vertical crenulation cleavage. (b) Conceptual model for the development of the Ibero-Armorican Arc in terms of sinistral transpression, folding and reorientaion of FS_3 fold trends, whereby the original FS_3 trends are preserved in porphyroblasts and other low strain zones (circles). (c) Aeromagnetic map apparently imaging a large S-shaped orocline whose south-eastern part is largely concealed by post-Palaeozoic cover.

belt (Fig. 12b). Pre-orocline trends may have been preserved in porphyroblasts and mesoscopic low-strain domains assuming that the bulk flow vorticity was strongly partitioned around these bodies (cf. Aerden, 1994, 1995). A similar model has been proposed for the Kimberly orocline of NW-Australia (Bell and Mares, 1999).

Although still very speculative at this stage, structural relationships in more southern regions of the Iberian Massif are apparently consistent with late-Variscan sinistral transpression (Fig. 12b). The asymmetric fold mapped by Díez Balda et al. (1995) can be interpreted in terms of late-stage E–W- to NW–SE folding and shearing having reoriented earlier fold trends. González Lodeiro (1981) showed that the main N–S-trending folds in the eastern part of the Spanish Central System are overprinted by weaker and younger WNW–SSE-trending folds. Julivert et al. (1983) describe dome-and-basin structures in low-grade rocks of the south-eastern part of the Iberian Massif that suggest younger WNW–SSE-trending folds superposed on older NE–SW-trending ones. Azor et al. (1994) describe late WNW–SSE-trending crenulation cleavages and sinistral faults superposed on earlier NNW–SSE-trending structures. Aeromagnetic data also suggest that fold patterns across the orocline probably interconnect in a large 'S'-shaped geometry partially concealed below post-Palaeozoic cover (Ardizone et al., 1988; Fig. 12c). This interpretation of the Iberian Massif is currently being tested against (micro)structural data from new samples.

9.3. Significance of fold-axes parallel stretching lineations in NW-Iberia

In the medium- to high-grade rocks of NW-Iberia, stretching lineations are mostly parallel to fold axes, whereas tectonic transport in more external orogenic zones was associated with thrusting transverse to the belt. According to the interpretations adopted in this paper, fold axes should have formed parallel to stretching lineations wherever the maximum stretching rate was oriented parallel to the FIA (Fig. 2a). For example, during contractional folding with horizontal stretching (lateral escape) of an originally horizontal foliation, or during gravitational collapse with lateral escape of an originally steeply dipping foliation. Conversely, non-cylindrical folds oblique to stretching lineations (e.g. sheath folds) should have formed wherever stretching directions were highly oblique to the FIA, for example, during contractional folding with vertical stretching of rocks previously containing a horizontal foliation, or during gravitational collapse of rocks originally containing a steeply dipping foliation with tectonic transport transverse to the strike of that foliation. Simultaneous activity of these different tectonic regimes in the Variscan orogen has been recently suggested in the Montagne Noire (French Massif Central), where bulk shortening and orogen-parallel stretching at deep crustal levels was coeval with low-angle thrusting transverse to the orogen at higher crustal levels (Aerden and Malavieille, 1999). This was interpreted in terms of gravitational spreading of a thrust wedge decoupled from a continuously converging footwall. A similar decoupling between bulk shortening in the footwall and low-angle thrusting in the hanging wall of a major detachment in NW-Iberia was also concluded by Gutiérrez Alonso (1996) and explains the contrasting tectonic transport directions in internal and external orogenic zones.

10. Conclusion

Inclusion trails preserved by progressive stages of porphyroblast growth in NW-Iberia can be grouped into four sets with distinctive strikes and consistent relative timing. This microstructural succession can be correlated with different fold generations recognised in the field, and is interpreted as a record of successive crustal shortening directions during the Variscan orogeny. Additional preferred vertical and horizontal orientations of the inclusion trails analysed are attributed to periodic gravitational instability during orogenesis, as independently documented earlier by other workers (e.g. Martínez Catalán et al., 1996; Escuder Viruete et al., 1994). The oldest recognised inclusion trails have consistent E–W trends and may relate to N–S oriented subduction (in present geographic coordinates) of the Gondwana margin during the upper Devonian–Carboniferou transition. Three subsequent directions of folding and thrusting produced a strongly curved orogen (Ibero-Armorican Arc) and large-scale fold interference structures, in a way already envisioned by Martínez et al., (1988). The orientation consistency between inclusion trails from 30 widely spaced samples representing both allochthonous and autochthonous tectonic units suggests some mechanism that suppressed porphyroblast rotation during bulk non-coaxial deformation. Otherwise, a succession of relatively coaxial deformations would have to be assumed, but this is unlikely considering that the majority of samples was collected from the strongly sheared base of the Iberian allochthonous complexes.

Acknowledgements

I am indebted to José-Ramón Martínez Catalán, Ricardo Arenas and Florentino Díaz García for sharing their knowledge of the Iberian Massif, help with collecting samples and many other matters. I also thank Antonia Díez Balda, Javier Escuder Viruete and Emilio González Clavijo for visits to their field areas and discussions. Angel Ramos González and Andrés Sánchez Boyero are thanked for the production of a large collection of excellent thin-sections at the University of Salamanca, and Pablo González Cuadra for providing sample 15. Careful referee reports from Scott Johnson, Aaron Stallard, and Fernando Ornelas Marques led to major clarification of original manuscript versions and are gratefully acknowledged. This research was funded by a post-doctoral grant from the Spanish government, a visiting lectureship at the University of Salamanca, and a DGICYT research project coordinated by José-Ramón Martínez Catalán.

References

Abalos, B., 1997. Omphacite fabric variation in the Cabo Ortegal Eclogite (NW Spain); relationships with strain symmetry during high-pressure deformation. Journal of Structural Geology 19, 621–637.

Aerden, D.G.A.M., 1994. Kinematics of orogenic collapse in the Variscan Pyrenees deduced from microstructures in porphyroblastic rocks from the Lys-Caillaouas Massif. Tectonophysics 236, 139–160.

Aerden, D.G.A.M., 1995. Porphyroblast non-rotation during crustal extension in the Variscan Pyrenees. Journal of Structural Geology 17, 709–726.

Aerden, D.G.A.M., 1998. Tectonic evolution of the Montagne Noire and a possible orogenic model for syn-collisional exhumation of deep rocks, Hercynian belt, France. Tectonics 17, 62–79.

Aerden, D.G.A.M., 2003. Preferred orientation of planar microstructures determined via statistical best-fit of measured intersection-lines: the 'FitPitch' computer program. Journal of Structural Geology, 25(6), 923–934.

Aerden, D.G.A.M., Malavieille, J., 1999. Origin of a large-scale fold nappe in the Montagne Noire (Variscan Belt, France). Journal of Structural Geology 21, 1321–1333.

Aller, J., Gallastegui, J., 1995. Analysis of kilometric-scale superposed folding in the Central Coal Basin (Cantabrian zone, NW Spain). Journal of Structural Geology 17, 961–969.

Ardizone, J., Mezcua, J., Socias, I., 1989. Mapa aeromagnético de España peninsular. Publicaciones de Geodesia y Geofisica. Dirección General del Instituto Geográfico Nacional (http://www.geo.ign.es/servidor/geom/aero/aero.html).

Arenas, R., Rubio Pascual, F., Díaz García, F., Martínez Catalán, J.R., 1995. High-pressure micro-inclusions and development of an inverted metamorphic gradient in the Santiago Schists (Ordenes Complex, NW Iberian Massif, Spain): evidence of subduction and syncollisional decompression. Journal of Metamorphic Geology 13, 141–164.

Azor, A., González Lodeiro, F., Simancas, J.F., 1994. Tectonic evolution of the boundary between the Central Iberian and Ossa Morena zones (Variscan belt, southwest Spain). Tectonics 13, 45–61.

Bell, T.H., 1985. Deformation partitioning and porphyroblast rotation in metamorphic rocks: A radical reinterpretation. Journal of Metamorphic Geology 3, 109–118.

Bell, T.H., Johnson, S.E., 1989. Porphyroblast inclusion trails: the key to orogenesis. Journal of Metamorphic Geology 7, 279–310.

Bell, T.H., Mares, V., 1999. Correlating deformation and metamorphism around orogenic arcs. American Mineralogist 84, 1727–1740.

Bell, T.H., Welch, P.W., 2002. Prolonged Acadian orogenesis: revelations from foliation intersection axis (FIA) controlled monazite dating of foliations in porphyroblasts and matrix. American Journal of Science 302, 549–581.

Bell, T.H., Johnson, S.E., Davis, B., Forde, A., Hayward, N., Wilkins, C., 1992. Porphyroblast inclusion trail data; eppure non son girate. Journal of Metamorphic Geology 10, 295–308.

Bell, T.H., Forde, A., Wang, J., 1995. A new indicator of movement direction during orogenesis: measurement technique and application to the Alps. Terra Nova 7, 500–508.

Bell, T.H., Hickey, K.A., Upton, G.J.G., 1999. Distinguishing and correlating multiple phases of metamorphism across a multiply deformed region using the axes of spiral, staircase, and sigmoidally curved inclusion trails in garnet. Journal of Metamorphic Geology 16, 767–794.

Brun, J.P., Burg, J.P., 1982. Combined thrusting and wrenching in the Ibero-Armorican Arc; a corner effect during continental collision. Earth and Planetary Science Letters 61 (2), 319–332.

Burg, J.P., Bale, P., Brun, J.P., Girardeau, J., 1987. Stretching lineations and transport direction in the Ibero-Armorican arc during the siluro-devonian collision. Geodinamica Acta 1, 71–81.

Dallmeyer, R.D., Martínez Catalán, J.R., Arenas, R., Gil Ibarguchi, J.I., Gutiérrez Alonso, G., Farias, P., Aller, J., 1997. Diachronous Variscan tectonothermal activity in the NW Iberian Massif: evidence from $^{40}Ar/^{39}Ar$ dating of regional fabrics. Tectonophysics 277, 307–337.

Dias, R., Ribeiro, A., 1995. The Ibero-Armorican Arc—a collision effect against an irregular continent. Tectonophysics 246, 113–128.

Díaz García, F., Martínez Catalán, J.R., Arenas, R., Gonzalez Cuadra, P., 1999. Structural and kinematic analysis of the Corredoiras Detachment; evidence for early Variscan synconvergent extension in the Ordenes Complex, NW Spain. International Journal of Earth Sciences 88, 337–351.

Díez Balda, M.A., Martínez Catalán, J.R., Ayarza Arribas, P., 1995. Syn-collisional extensional collapse parallel to the orogenic trend in a domain of steep tectonics: the Salamanca Detachment Zone (Central Iberian Zone, Spain). Journal of Structural Geology 17, 163–182.

Engels, J.P., 1972. The catazonal polymetamorphic rocks of Cabo Ortegal (NW Spain), a structural and petrofabric study. Leidse Geologische Mededelingen 48, 83–133.

Escuder Viruete, J., Arenas, R., Martínez Catalán, J.R., 1994. Tectonothermal evolution associated with Variscan crustal extension in the Tormes Gneiss Dome (NW Salamanca, Iberian Massif, Spain). Tectonophysics 238, 117–138.

Escuder Viruete, J., Hernaiz Huerta, P.P., Valverde Vaquero, P., Rodriguez Fernandez, R., Dunning, G., 1998. Variscan syncollisional extension in the Iberian Massif; structural, metamorphic and geochronological evidence from the Somosierra sector of the Sierra de Guadarrama (Central Iberian Zone, Spain). Tectonophysics 290, 87–109.

Galibert, F., 1984. Géochimie et géochronologie du complexe granitique de l'antiforme de Morille (Salamanque, Espagne). Unpublished D.E.A. rapport, Laboratoire de Géochimie Isotopique, Université de Montpellier, 53pp.

González Lodeiro, F., 1981. Posicion de las series infraordovicicas en el extremo oriental del Sistema Central y su correlacion. Cuadernos del Laboratorio Geologico de Laxe 2, 125–134.

Gutiérrez Alonso, G., 1996. Strain partitioning in the footwall of the Somiedo Nappe: structural evolution of the Narcea Tectonic Window, NW Spain. Journal of Structural Geology 18, 1217–1229.

Hayward, N., 1990. Determination of early fold axis orientations within multiply deformed rocks using porphyroblasts. Tectonophysics 179, 353–369.

Hayward, N., 1992. Microstructural analysis of the classical spiral garnet porphyroblasts of south-east Vermont: evidence for non-rotation. Journal of Metamorphic Geology 10, 567–587.

Hickey, K.A., Bell, T.H., 1999. Behaviour of rigid objects during deformation and metamorphism: a test using schists from the Bolton syncline, Connecticut, USA. Journal of Metamorphic Geology 17, 211–228.

Jiang, D., 2001. Reading history of folding from porphyroblasts. Journal of Structural Geology 23, 1327–1335.

Johnson, S.E., 1990. Deformation history of the Otago schists, New Zealand, from progressively developed porphyroblast-matrix microstructures: uplift-collapse orogenesis and its implications. Journal of Structural Geology 12, 727–746.

Johnson, S.E., 1992. Sequential porphyroblast growth during progressive deformation and low-P high-T (LPHT) metamorphism, Cooma Complex, Australia; the use of microstructural analysis to better understand deformation and metamorphic histories deformation and metamorphic histories. Tectonophysics 214, 311–340.

Johnson, S.E., 1999. Near-orthogonal foliation development in orogens: meaningless complexity, or reflection of fundamental dynamic processes? Journal of Structural Geology 21, 1183–1187.

Julivert, M., Arboleya, M.L., 1984. A geometrical and kinematical approach to the nappe structure in an arcuate fold belt; the Cantabrian nappes (Hercynian chain, NW Spain). Journal of Structural Geology 6, 499–519.

Julivert, M., Marcos, A., 1973. Superimposed folding and flexural conditions in the Cantabrian Zone (Hercynian Cordillera, NW Spain). American Journal of Science 273, 353–375.

Julivert, M., Vegas, R., Roiz, J.M., Martínez Rius, A., 1983. La estructura de la extension SE de la Zona Centro-Iberica con metamorfismo de bajo grado. In: Libro Jubilar, J.M., (Ed.), Rios—Geologia de España I, Instituto Geologico y Minero de España, Madrid, pp. 339–380.

Jung, W.S., Ree, J.H., Park, Y., 1999. Non-rotation of garnet porphyroblasts and 3-D inclusion trail data: an example from the Imjingang belt, South Korea. Tectonophysics 307, 381–395.

Lefort, J.P., Agarwal, B.N.P., 1999. Of what is the centre of the Ibero-Armorican arc composed? Tectonophysics 302, 71–81.

Marcos, A., 2000. On field relations between high-grade rocks in the Cabo Ortegal Complex (Variscan orogen, NW Spain) and their implications on the lithological sequence and structure. In: Variscan–Appallachian dynamics: the building of the Upper Palaeozoic basement. Basement Tectonics 15, La Coruña, Spain, Programs and Abstracts 7.

Marques, F.G., Ribeiro, A., Perivia, E., 1992. Tectonic evolution of the deep crust: Variscan reactivation by extension and thrusting of pre-Cambrian basement in the Bragança and Morais Massifs. Geodinamica Acta 5, 135–151.

Martínez, F.J., Julivert, M., Sebastian, A., Arboleya, M.L., Gil-Ibarguchi, J.I., 1988. Structural and thermal evolution of high-grade areas in the north-western parts of the Iberian Massif. American Journal of Science 288, 969–996.

Martínez Catalán, J.R., Arenas, R., Díaz García, F., Rubio Pascual, F.J., Abati, J., Marquínez, J., 1996. Variscan exhumation of a subducted Palaeozoic continental margin: the basal units of the Ordenes Complex, Galicia, NW Spain. Tectonics 15, 106–121.

Martínez García, E., 1973. Deformacion y metamorfismo en la zona de Sanabria (Provincias de Zamora, León y Orense, Noroeste de España). Studia Geologica, Universidad de Salamanca 5, 7–106.

Matte, P., 1991. Accretionary history and crustal evolution of the Variscan belt in western Europe. Tectonophysics 196, 309–337.

Matte, P., 2001. The Variscan collage and orogeny (480–290 Ma) and the tectonic definition of the Armorica microplate: a review. Terra Nova 13, 122–128.

Pérez Estaún, A., Bastida, F., Alonso, J.L., Marquinez, J., Aller, J., Alvarez Marron, J., Marcos, A., Pulgar, J.A., 1988. A thin-skinned tectonic model for an arcuate fold and thrust belt: the Cantabrian Zone (Variscan Ibero-Armorican Arc). Tectonics 7, 517–537.

Ribeiro, A., 1974. Contribution à L'Etude Tectonique de Trás-os-Montes Oriental. Published Ph.D. thesis, Serv. Geol. Portugal, Memória 24 (Nova Série), 168pp.

Ribeiro, A., Pereira, E., Dias, R., 1990. Allochthonous sequences. In: Dallmeyer, R.D., Martínez García, E. (Eds.), Pre-Mesozoic Geology of Iberia, Springer-Verlag, New York, pp. 220–236.

Ries, A.C., Shackleton, R.M., 1976. Patterns of strain variation in arcuate fold belts. Philosophical Transactions of the Royal Society of London A 283, 281–288.

Santos Zalduegui, J.F., Schrärer, U., Gil Ibarguchi, J.I., 1995. Isotope constraints on the age and origin of magmatism and metamorphism in the Malpica-Tuy allochthon Galicia, NW-Spain. Chemical Geology 121, 91–103.

Stallard, A., 1998. Episodic porphyroblast growth in the Fleur de Lys Supergroup, Newfoundland; timing relative to the sequential development of multiple crenulation cleavages. Journal of Metamorphic Geology 16, 711–728.

Stallard, A., Hickey, K., 2001. Shear zone vs. folding origin for spiral inclusion trails in the Canton Schist. Journal of Structural Geology 23, 1845–1864.

Takeda, Y.T., 2001. Partitioning of vorticity in bimineralic rocks. Journal of Structural Geology 23, 1319–1324.

Van Calsteren, P.W.C., Boelrijk, N.A.I.M., Hebeda, E.H., Priem, H.N.A., Den Tex, E., Verdurmen, E.A.T.H., Verschure, R.H., 1979. Isotopic dating of older elements (including the Cabo-Ortegal mafic-ultramafic complex) in the Hercynian orogen of NW Spain: manifestations of a presumed early-Palaeozoic mantle plume. Chemical Geology 24, 35–56.

Van der Voo, R., Stamatakos, J.A., Pares, J.M., 1997. Kinematic constraints on thrust-belt curvature from syndeformational magnetizations in the Lagos del Valle Syncline in the Cantabrian Arc, Spain. Journal of Geophysical Research B 102, 105–119.

Van Zuuren, A., 1969. Structural petrology of an area near Santiago de Compostella (NW Spain). Leidse Geologische Mededelingen 45, 1–71.

Weil, A.B., Van der Voo, R., van der Pluijm, B.A., Parés, J.M., 2000. The formation of an orocline by multiphase deformation: a paleomagnetic investigation of the Cantabria-Asturias Arc (northern Spain). Journal of Structural Geology 22, 735–757.

Williams, P.F., Jiang, D., 1999. Rotating garnets. Journal of Metamorphic Geology 17, 367–378.